7-1-1999

Different Proctolin Neurons Elicit Distinct Motor Patterns From a Multifunctional Neuronal Network

Dawn M. Blitz
Miami University

Andrew E. Christie

Melissa J. Coleman
Claremont McKenna College; Pitzer College; Scripps College

Brian J. Norris

Eve Marder
Brandeis University

See next page for additional authors

Recommended Citation

Blitz, Dawn M., Andrew E. Christie, Melissa J. Coleman, Brian J. Norris, Eve Marder, and Michael P. Nusbaum. "Different Proctolin Neurons Elicit Distinct Motor Patterns from a Multifunctional Neuronal Network." The Journal of Neuroscience 19.13 (1999): 5449-5463.

Authors

Dawn M. Blitz, Andrew E. Christie, Melissa J. Coleman, Brian J. Norris, Eve Marder, and Michael P. Nusbaum

Different Proctolin Neurons Elicit Distinct Motor Patterns from a Multifunctional Neuronal Network

Dawn M. Blitz,[1] **Andrew E. Christie,**[1,2] **Melissa J. Coleman,**[1] **Brian J. Norris,**[1] **Eve Marder,**[2] **and Michael P. Nusbaum**[1]

[1]*Department of Neuroscience, University of Pennsylvania School of Medicine, Philadelphia, Pennsylvania 19104-6074, and* [2]*Volen Center for Complex Systems, Brandeis University, Waltham, Massachusetts 02454*

Distinct motor patterns are selected from a multifunctional neuronal network by activation of different modulatory projection neurons. Subsets of these projection neurons can contain the same neuromodulator(s), yet little is known about the relative influence of such neurons on network activity. We have addressed this issue in the stomatogastric nervous system of the crab *Cancer borealis*. Within this system, there is a neuronal network in the stomatogastric ganglion (STG) that produces many versions of the pyloric and gastric mill rhythms. These different rhythms result from activation of different projection neurons that innervate the STG from neighboring ganglia and modulate STG network activity. Three pairs of these projection neurons contain the neuropeptide proctolin. These include the previously identified modulatory proctolin neuron and modulatory commissural neuron 1 (MCN1) and the newly identified modulatory commissural neuron 7 (MCN7). We document here that each of these neurons contains a unique complement of cotransmitters and that each of these neurons elicits a distinct version of the pyloric motor pattern. Moreover, only one of them (MCN1) also elicits a gastric mill rhythm. The MCN7-elicited pyloric rhythm includes a pivotal switch by one STG network neuron from playing a minor to a major role in motor pattern generation. Therefore, modulatory neurons that share a peptide transmitter can elicit distinct motor patterns from a common target network.

Key words: stomatogastric nervous system; crustacea; projection neurons; neuromodulation; Cancer borealis*; central pattern generators*

Many neuronal networks produce multiple motor patterns (Marder and Calabrese, 1996), in part because of activity of different modulatory projection neurons (Norris et al., 1996; Perrins and Weiss, 1996; Blitz and Nusbaum, 1997). However, in many systems it is difficult to record from these neurons. Even in the systems in which such studies are undertaken, only some projection neurons have had their transmitter(s) identified (Kuhlman et al., 1985; Nusbaum and Kristan, 1986; Nusbaum and Marder, 1989a; Thorogood and Brodfuehrer, 1995; Norekian and Satterlie, 1996; McCrohan and Croll, 1997). Consequently, little is known about whether multiple projection neurons with a common modulatory transmitter influence a neural network in the same manner. Results from studies using exogenously applied neuromodulators, pharmacology, and/or stimulation of neuronal populations suggest a unified role for same transmitter-containing neurons in their influence on network activity (McCormick, 1992;

Aston-Jones et al., 1996; Page and Sofroniew, 1996; Edwards and Kravitz, 1997; Jacobs and Fornal, 1997).

Projection neurons that share a neuromodulator might elicit different responses from the same network because of the influence of distinct cotransmitters. The presence of cotransmitters is ubiquitous throughout all nervous systems (Weiss et al., 1993; Lundberg, 1996; Brezina and Weiss, 1997). It is also possible that a shared neuromodulator will affect a network in different ways when released by distinct modulatory neurons, even in the absence of different cotransmitters. For neuropeptide transmitters, this could result from a compartmentalization of their actions, as would occur if their range of influence was limited by extracellular peptidases (Sigvardt et al., 1986; Coleman et al., 1994; Saleh et al., 1996) or if they were released either at different distances from their receptors or in different amounts (Vilim et al., 1996).

These issues can be studied in the crustacean stomatogastric nervous system (STNS) (Harris-Warrick et al., 1992a; Marder et al., 1997). This nervous system consists of the stomatogastric ganglion (STG), esophageal ganglion (OG) and commissural ganglia (CoGs), plus their connecting and motor nerves. Overlapping subsets of STG neurons generate the gastric mill and pyloric rhythms, which control the chewing and filtering behaviors of the foregut, respectively (Weimann et al., 1991; Heinzel et al., 1993; Weimann and Marder, 1994). In the crab *Cancer borealis*, ~20 pairs of projection neurons innervate the STG, most of which originate in the CoGs and OG (Coleman et al., 1992).

Here, we show that three modulatory projection neurons that innervate the STG contain the same peptide transmitter, proctolin, but each one has a distinct complement of cotransmitters. Moreover, under the same conditions, they each elicit distinct motor patterns from the STG neural network. This appears to

result from the different cellular and synaptic mechanisms that each proctolin neuron uses for motor pattern selection, including their use of distinct cotransmitter complements.

Some of this work has appeared previously in abstract form (Nusbaum et al., 1989; Christie et al., 1993; Coleman et al., 1993).

MATERIALS AND METHODS

Animals. Crabs, *C. borealis*, were obtained from commercial suppliers (Boston, MA) and the Marine Biological Laboratory (Woods Hole, MA). Animals were maintained in aerated artificial seawater at 10–12°C, and were cold-anesthetized by packing in ice for 20–40 min before dissection. The stomach, including the STNS, was removed from the animal, and the rest of the dissection was performed in chilled (~4°C) physiological saline. Data were obtained from 190 male crabs.

Solutions. *C. borealis* physiological saline had the following composition (in mM): NaCl, 440; MgCl$_2$, 26; CaCl$_2$, 13; KCl, 11; Trizma base, 10; and maleic acid, 5, pH 7.4–7.6.

Immunocytochemistry. Whole-mount immunocytochemistry was performed using standard techniques for this system (Beltz and Kravitz, 1983; Blitz et al., 1995). Briefly, tissue was fixed for 2–24 hr with either 4% paraformaldehyde or 4% 1-ethyl 3-(3 dimethylaminopropyl)-carbodiimide (EDAC; Sigma, St Louis, MO) in 0.1 M sodium phosphate, pH 7.3. Preparations were then rinsed five times at 1 hr intervals in 0.1 M sodium phosphate (P) with 0.3% Triton X-100 (P-Triton, pH 7.3). Tissue was incubated with primary antibodies for 24–96 hr. Primary antibodies were used at a final dilution of 1:300–1:1500 (see below). In each case, the primary antibody was diluted with P-Triton. The tissue was then rinsed as above and incubated for 15–24 hr with goat anti-rat, goat anti-mouse, and/or goat anti-rabbit secondary antibodies conjugated to rhodamine or fluorescein (Calbiochem, San Diego, CA; Boehringer Mannheim, Indianapolis, IN). The secondary antibody was used at a final dilution of 1:25–1:300 in P-Triton. Preparations were then rinsed five times at 1 hr intervals with P. They were then mounted between a glass slide and coverslip with a solution of 80% glycerol and 20% 20 mM Na$_2$CO$_3$, pH 9.0.

Whole mounts of the STNS were viewed, and images were collected using either a Bio-Rad (Hercules, CA) MRC 600 or a Leica (Nussloch, Germany) TCS_NT laser scanning confocal microscope. The Bio-Rad system was equipped with a Zeiss (Thornwood, NY) Axioskop microscope and a krypton-argon mixed gas laser plus the Bio-Rad K1 (488 and 560 nm dual excitation, dual dichroic reflector) and K2 (dichroic, DR 560 LP; green emission filter, 522 nm DF35; red emission filter, 585 nm, EFLP) filter sets. The Bio-Rad-supplied Comos software was used for collecting all images with this system. The Leica TCS_NT system was equipped with a Leica DMRBE microscope plus a krypton-argon mixed gas laser. A standard Leica supplied FITC-TRITC filter set (DD488/568, RSP 580, BF530/30, LP 590) and Leica TCS_NT software were used to collect images with this system.

Data analysis was done on either single optical sections or by combining the sections into pseudo-colored composite images or stereo pair images. Sections were combined using a "maximum projection" program provided by either the Comos software or the Leica TCS_NT software. To determine whether an immunoreactivity was contained within a filled structure or whether two immunoreactivities were colocalized to a single profile, high-magnification images of each dye or label were collected simultaneously from the same focal plane. Single optical sections, as well as Z-series stacks were collected for each dye or immunoreactivity. Simultaneously collected images were merged with either Comos or TCS_NT software. By pseudocoloring the images red for rhodamine and green for either Lucifer yellow or fluorescein, regions of overlap were revealed in both programs as structures colored yellow. Pixel sizes for these images ranged from ~0.1 to 0.2 μm/pixel. Confocal micrographs were printed using either a Sony (Tokyo, Japan) Mavigraph color video printer or a Tektronix (Wilsonville, OR) Phaser II dye sublimation printer.

All of the primary antibodies used in this study have been used previously in the crustacean STNS and/or other crustacean tissues, and the specificity of these antibodies has been characterized. Proctolin immunoreactivity was detected with three polyclonal proctolin antibodies, provided by Drs. C. Bishop and M. O' Shea (University of Sussex, Sussex, UK; proctolin$_{BO}$) (Bishop et al., 1981), Dr. N. Davis (University of Arizona, Tucson, AZ; proctolin$_{ND}$) (Davis et al., 1989), and Dr. H. Agricola (Friedrich-Schiller-Universitat, Jena, Germany; proctolin$_{HA}$). The first two were used at 1:300, and the latter one was used at 1:1500.

The proctolin$_{HA}$ antibody labeling within the STNS is indistinguishable from that seen with the proctolin$_{ND}$ and proctolin$_{BO}$ antibodies (A. E. Christie, D. M. Blitz, and M. P. Nusbaum, unpublished observations) (Marder et al., 1986). Marder et al. (1986) showed that the proctolin immunoreactivity in the STNS is associated with a substance that is chromatographically indistinguishable from native proctolin (amino acid sequence RYLPT). Tachykinin-related peptide (TRP) immunoreactivity was examined using a rat monoclonal antibody generated against substance P (Accurate Chemicals, Westbury, NY) (Goldberg et al., 1988) used at 1:300. This antibody cross-reacts with the native TRP in the crab STNS, called *C. borealis* tachykinin-related peptide Ia (CabTRP Ia; APSGFLGMRamide) (Blitz et al., 1995; Christie et al., 1997a). GABA immunoreactivity was examined using a rabbit polyclonal antibody (Sigma) used at 1:200–1:500 (Christie, 1995). Preadsorption controls for GABA immunolabeling in the STNS are described below. Two rabbit polyclonal antibodies generated against FMRFamide were used, including one from INCSTAR Corp. (Stillwater, MN) (Schmidt and Ache, 1994) and FMRFamide antibody 671 (Marder et al., 1987). Both were used at 1:300. Weimann et al. (1993) demonstrated that the major native FMRFamide-like molecules in *C. borealis* are extended FLRFamide peptides (SDRNFLRFamide and TNRNFLRFamide). To detect histamine-like immunoreactivity, a rabbit polyclonal antibody generated against histamine (Accurate Chemicals) (Mulloney and Hall, 1991) was used. This antibody required the use of an EDAC fixative (see above) and was used at 1:500 (Christie, 1995). Red pigment concentrating hormone-like immunoreactivity was detected using a rabbit polyclonal antiserum (Dr. R. Elde, University of Minnesota, Minneapolis, MN) (Madsen et al., 1985; Nusbaum and Marder, 1988) used at 1:200. Allatostatin-like immunoreactivity was examined using a rabbit polyclonal antibody at 1:500 (Dr. H. Agricola) (Skiebe and Schneider, 1994).

Preadsorption controls. To confirm that the GABA-like immunoreactivity seen in the crab stomatogastric nervous system was attributable to the presence of the anti-GABA antibodies and not an unknown contaminant in the antiserum, we conducted a series of preadsorption controls. The polyclonal anti-GABA antiserum used in our study was generated in rabbit against a GABA-bovine serum albumin (BSA) conjugate. Thus, we used either GABA-BSA conjugate or unconjugated BSA as a blocking agent in our preadsorption controls. The GABA-BSA conjugate used in our study was generated via a glutaraldehyde cross-linking reaction (Protein Chemistry Laboratory, Cancer Research Center, University of Pennsylvania). In each blocking experiment, the anti-GABA antiserum (1:200 final dilution) was incubated with either GABA-BSA conjugate or unconjugated BSA for 2 hr at room temperature (~20°C) before incubation with the stomatogastric nervous system. Incubation of the GABA antiserum with GABA-BSA conjugate (10^{-7} M) completely abolished GABA immunolabeling throughout the stomatogastric nervous system ($n = 4$ of 4 preparations; data not shown). In contrast, GABA immunolabeling in preparations in which the antiserum was preincubated with unconjugated BSA (10^{-7} M; $n = 4$ of 4 preparations) was no different from immunolabeling after preincubations at room temperature with no blocking agent present.

Intracellular dye fills. Microelectrodes used for dye injections had resistances of 50–70 MΩ. The electrode tip was filled with either 5% Lucifer yellow CH dilithium salt (LY; Sigma) in distilled water or 10% lysine-fixable, anionic rhodamine-dextran, molecular weight 3000 (Molecular Probes, Eugene, OR) in distilled water. The electrode was backfilled with 1 M lithium chloride with an air bubble between the dye and lithium chloride solutions. Dye was injected into neuronal somata via hyperpolarizing current pulses (current, −5 nA; rate, 1 Hz; duty cycle, 0.5) through the electrode for 15–60 min. Intracellular fills of the STG arbor of modulatory commissural neuron 1 (MCN1) were done using DC hyperpolarizing current injection (−2 to −5 nA) for 15–60 min into the stomatogastric nerve axon (SNAX) of MCN1 (MCN1$_{SNAX}$; Coleman and Nusbaum, 1994).

Electrophysiology. Electrophysiological experiments were performed using standard techniques for this system (Bartos and Nusbaum, 1997). The isolated STNS (Fig. 1) was pinned down in a SYLGARD 184 (KR Anderson, Santa Clara, CA)-lined Petri dish. All preparations were superfused continuously with *C. borealis* physiological saline (10–13°C). Extracellular recordings were made by pressing stainless steel pin electrodes into the SYLGARD alongside the nerves and isolating each area with Vaseline. The desheathed ganglia were viewed with light transmitted through a dark-field condenser (Nikon, Tokyo, Japan) to facilitate intracellular recordings. Intracellular recordings of STG, OG, and CoG somata were made using microelectrodes (15–30 MΩ) filled with 4 M

potassium acetate plus 20 mM potassium chloride. Intracellular current injection was performed using Axoclamp 2 amplifiers (Axon Instruments, Foster City, CA) in single-electrode discontinuous current-clamp (DCC) mode. Sample rates during DCC were 2–3 kHz. In some preparations, MCN1 was stimulated extracellularly via the inferior esophageal nerve (*ion*; 10–30 Hz) (Bartos and Nusbaum, 1997). The ion was stimulated using a Grass S88 stimulator and Grass SIU5 stimulus isolation unit (Astro-Med/Grass Instruments, Warwick, RI). Data were collected on an MT-95000 chart recorder (Astro-Med/Grass Instruments) and videotape (Vetter Instruments, Rebersburg, PA).

STG neurons were identified on the basis of their axonal projections, their activity patterns, and their interactions with other STG neurons (Weimann et al., 1991; Norris et al., 1996; Bartos and Nusbaum, 1997). Projection neurons were identified by their soma location, axonal projection, and influence on the STG network (Nusbaum and Marder, 1989a; Coleman and Nusbaum, 1994; Norris et al., 1994; Blitz and Nusbaum, 1997).

Data. In measuring pyloric cycle frequency for modulatory proctolin neuron (MPN) and MCN7 stimulations, the mean of 10 consecutive pyloric cycles before and during stimulation were compared. A pyloric cycle is arbitrarily defined as extending from the start of one pyloric dilator (PD) neuron burst to the start of the next PD burst. During MCN1 stimulations, the pyloric cycle frequency was measured separately during each of the two phases of the gastric mill rhythm, including the retraction [dorsal gastric (DG) neuron] and protraction [lateral gastric (LG) neuron] phases. The pyloric cycle frequency during DG and LG phases was determined from the mean pyloric cycle frequency during four consecutive DG and LG bursts and compared with the mean pyloric cycle frequency from 10 consecutive pyloric cycles before stimulation (Bartos and Nusbaum, 1997).

Phase analysis was performed on data collected from four preparations for each condition. Phase is defined as the latency to occurrence of an event relative to the start of a cycle, divided by the cycle period. Thus, the onset and offset of activity in each neuron after the onset of a PD neuron burst were measured as a fraction of the total cycle duration. For saline and MPN stimulation, the average of 10 consecutive cycles from each preparation was taken. For MCN1 stimulation, pyloric cycles were categorized based on whether they occurred during a DG or LG neuron burst. The average of 10 cycles during consecutive DG bursts and 10 cycles during consecutive LG bursts from each preparation were measured. For MCN7 stimulation, pyloric cycles were categorized as long- or short-duration cycles. The mean duration of 10 consecutive pyloric cycles was measured before each MCN7 stimulation. Short duration cycles were then defined as those shorter than one SD above the mean control pyloric cycle duration. Long-duration cycles were defined as those longer than 1 SD above the mean control duration. The averages of 10 short-duration and 10 long-duration cycles were measured from each preparation.

Statistical significance was determined using paired Student's *t* test, performed with SigmaPlot for Windows (version 4.0) and one-way repeated measures ANOVA or one-way ANOVA and the Tukey *t* test performed with SigmaStat for Windows (version 2.0). Data are expressed as mean ± SD. Figures were made by scanning data with a Hewlett–Packard (Palo Alto, CA) ScanJet IIC scanner, using DeskScan II (version 2.00a) software. Final figures were produced using CorelDraw (version 3.0 for Windows) or Adobe Photoshop (version 3.0.1 for Silicon Graphics).

RESULTS

Anatomy

Using immunocytochemistry paired with dye back-fills of the STG input nerve, Coleman et al. (1992) demonstrated that there are three pairs of proctolinergic neurons that project to the STG. No STG neurons contain proctolin (Marder et al., 1986; Coleman et al., 1992). Two of the proctolin neuron pairs originate in the CoGs, whereas the third pair originates in the OG. Previous work identified the OG pair of proctolin neurons as the MPNs (Fig. 1*A*) (Nusbaum and Marder, 1989a). In this study we show that another previously identified neuron pair (MCN1; Fig. 1*B*) (Coleman and Nusbaum, 1994) is proctolin-immunoreactive. We also identify and characterize the third proctolinergic neuron that innervates the STG (MCN7; Fig. 1*B*).
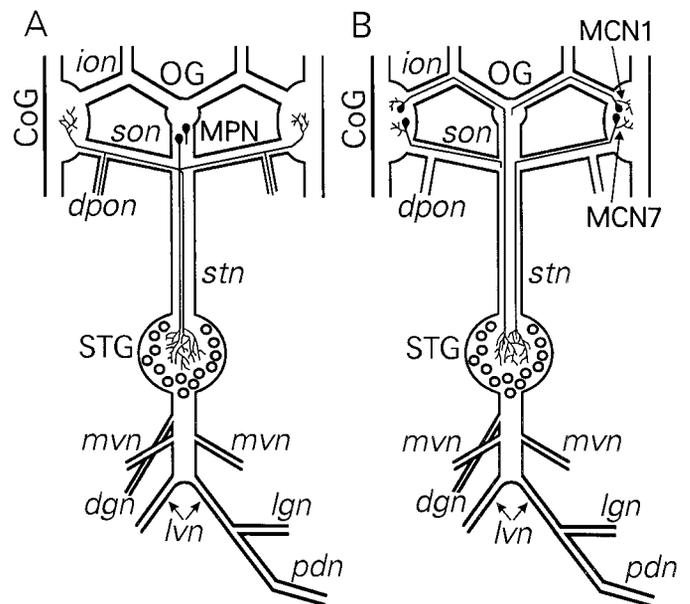
Figure 1. Schematics of the stomatogastric nervous system, including somata location and axonal pathways of the proctolin projection neurons MPN, MCN1, and MCN7. *A*, There is a pair of MPN somata located either in the OG or in the nerve posterior to this ganglion. Each MPN projects an axon through each *son* to the CoG and two axonal branches through the *stn* to the STG. It also projects an axonal branch from each *son* through the peripheral nerve *dpon*. For clarity, the complete projection of only one MPN is shown. *B*, There is a single MCN1 and MCN7 in each CoG. Each MCN1 projects an axon through the *ion* and *stn* to the STG. Each MCN7 projects an axon through the *son* and *stn* to the STG. For clarity, the complete projection of only one MCN1 and one MCN7 is shown. Ganglia; *CoG*, commissural ganglion; *OG*, esophageal ganglion; *STG*, stomatogastric ganglion; nerves: *dgn*, dorsal gastric nerve; *dpon*, dorsal posterior esophageal nerve; *ion*, inferior esophageal nerve; *lgn*, lateral gastric nerve; *lvn*, lateral ventricular nerve; *mvn*, medial ventricular nerve; *pdn*, pyloric dilator nerve; *son*, superior esophageal nerve; *stn*, stomatogastric nerve; neurons: *MCN1*, modulatory commissural neuron 1; *MCN7*, modulatory commissural neuron 7; *MPN*, modulatory proctolin neuron. Anterior is toward the *top*, and posterior is toward the *bottom*.

Identification of MCN7

Coleman et al. (1992) demonstrated that there is a single proctolinergic neuron that projects from each CoG to the STG via the superior esophageal nerve (*son*). Here, we document via intracellular recordings and double labeling experiments that a CoG neuron that we have designated MCN7 is the proctolin neuron that projects to the STG via the *son*. There is a single MCN7 in each CoG (Fig. 1*B*). In 60 CoGs, we found only one neuron per CoG with the projection pathway and influence on the STG network that we describe below for MCN7. Each MCN7 has a soma and neuropilar arborization in the CoG and projects an axon through the *son* (Fig. 2*A*). The MCN7 soma is located on the dorsal surface, usually anteromedially, and has a maximal cross-sectional diameter of 41.3 ± 2.1 μm (*n* = 4). Extending from the soma is a thin neurite (3.2 ± 0.5 μm; *n* = 4) that expands into a larger-diameter neurite (18.7 ± 2.3 μm; *n* = 4) from which arise all of the smaller neuropilar processes. The neurite then decreases in diameter (5.0 ± 2.3 μm; *n* = 4) as it exits the neuropil and enters the *son*. This anatomy is similar to that of other identified CoG projection neurons (Coleman and Nusbaum, 1994; Norris et al., 1994, 1996). Simultaneous intracellular recordings from the MCN7 soma and extracellular recordings of the *son* and the stomatogastric nerve (*stn*) show that each action
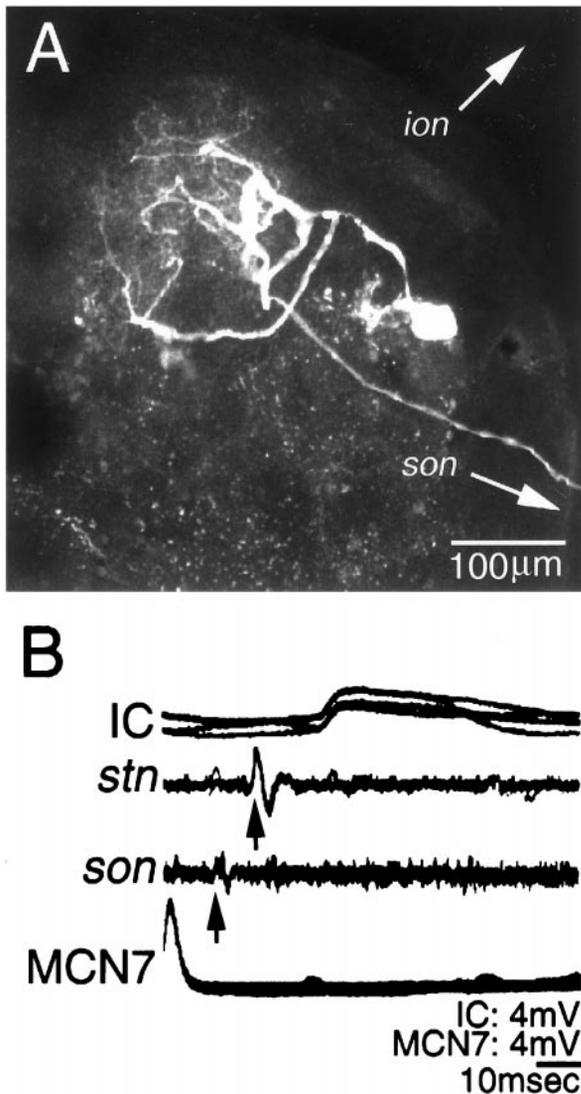
Figure 2. Anatomy and projection pathway of MCN7. *A,* Confocal image of a LY intracellular fill of MCN7 in the CoG. Anterior is toward the *top*, and medial is toward the *right*. A thin neurite projects from the MCN7 soma. It expands into a larger neurite, from which the fine processes arise. The neurite diameter is reduced again to form the axon, which leaves the CoG via the *son*. The image is a confocal composite of 24 optical sections collected at ~2 μm intervals. *B,* Overlaid oscilloscope traces were triggered by MCN7 action potentials elicited by injection of depolarizing current into its soma. Constant latency action potentials were recorded in the *son* and *stn* (*arrows*), followed by a constant latency postsynaptic potential in the IC neuron, an STG network neuron.

potential elicited in the MCN7 soma occurred, with a constant latency, first in the *son* and then in the *stn* ($n = 4$) (Fig. 2B). After the action potential in the *stn*, a time-locked EPSP was elicited in an STG neuron, the inferior cardiac (IC) neuron ($n = 4$) (Fig. 2B), demonstrating that MCN7 projects directly to the STG.

MCN1 cotransmitter complement

There is a single MCN1 in each commissural ganglion. This neuron projects through the *ion* and *stn* to innervate the STG (Fig. 1B) (Coleman and Nusbaum, 1994). Each MCN1 arborizes within the CoG as well as within the STG. Intracellular LY fills of MCN1 paired with proctolin immunocytochemistry demonstrated that this neuron is proctolin-immunoreactive within the CoG ($n = 13$) (Fig. 3A, Table 1). Pairing intrasomatic LY fills of

MCN1 with GABA immunocytochemistry demonstrated that MCN1 is also GABA-immunoreactive in the CoG ($n = 4$) (Fig. 3B, Table 1). We found that MCN1 also contains the peptide CabTRP Ia in its CoG arbor ($n = 5$) (Fig. 3C, Table 1).

At the entrance to the STG, the MCN1 axon is relatively large (~10 μm) and can be recorded intracellularly (Nusbaum et al., 1992; Coleman and Nusbaum, 1994). Previous work demonstrated that the STG and CoG arbors of MCN1 can be functionally compartmentalized (Coleman and Nusbaum, 1994). Thus, we wanted to determine whether the transmitter complements of the MCN1 arbors in the CoG and STG were also distinct. To this end, we filled the STG arbor of MCN1 (MCN1$_{SNAX}$) with LY and used immunocytochemistry to examine the MCN1 transmitter complement in its STG arbor. We found that, within the STG, MCN1 processes exhibit the same complement of immunolabeling as occurs in its CoG arbor, namely proctolin (Fig. 3D; $n = 10$), GABA (Fig. 3E; $n = 4$), and CabTRP Ia (Fig. 3F; $n = 12$).

All of the CabTRP Ia immunoreactivity within the STG is contained in the arbors of only two projection neurons (Goldberg et al., 1988; Blitz et al., 1995), which we now know to be the two MCN1 neurons. To determine whether MCN1$_{SNAX}$ was also immunoreactive for additional transmitters, we conducted double-labeling experiments in the STG neuropil in which we paired CabTRP Ia immunoreactivity with other antisera. We found that MCN1$_{SNAX}$ is not immunoreactive for histamine-like ($n = 4$), red pigment-concentrating hormone-like ($n = 4$), or allatostatin-like ($n = 4$) transmitters. We also paired intracellular LY fills of MCN1$_{SNAX}$ with FMRFamide immunocytochemistry and determined that MCN1$_{SNAX}$ is not FMRFamide immunoreactive ($n = 4$). Christie et al. (1997c) demonstrated that MCN1$_{SNAX}$ also exhibits no cholecystokinin-like immunoreactivity. MCN1$_{SNAX}$ is not serotonergic, because all of the serotonin (5-HT) immunoreactivity within the crab STG arises from the arbors of identified sensory neurons (Katz et al., 1989).

MPN cotransmitter complement

The two MPN neurons are most commonly located in the esophageal nerve (*on*), posterior to the OG (Nusbaum and Marder, 1989a). MPN projects axonal branches through the *stn* to the STG and through each *son* to each CoG (Fig. 1A). Nusbaum and Marder (1989a) demonstrated that MPN is proctolin-immunoreactive. Shown in Figure 4A is an intracellular LY fill of one MPN. The characteristic teardrop-shaped soma is evident in the *on*. In this preparation, both MPNs were physiologically identified and their position was noted, but the second one was not filled with LY. The nervous system was then processed for GABA immunocytochemistry, revealing GABA immunoreactivity in the two MPN neurons (Fig. 4B). The characteristic location of MPN allows these neurons to be identified on the basis of their anatomical location without previous physiological identification and intracellular dye filling. Thus, immunocytochemistry alone is sufficient to determine whether these neurons are likely to contain a particular neurotransmitter. Therefore, we demonstrated in other preparations that the MPNs are GABA-immunoreactive using only immunocytochemistry (Table 1). In 20 of 23 preparations, both MPNs were located in the *on* and were GABA-immunoreactive. In the remaining preparations there was either one MPN located in the *on* ($n = 2$ of 3) or no GABA immunoreactivity in the OG/*on* ($n = 1$ of 3).

Previous immunocytochemical studies have characterized the pattern of immunoreactivity within the STNS for several neurotransmitters (Marder et al., 1997). Based on the distinct location

MCN1: CoG Arbor   MCN1: STG Arbor

Proctolin
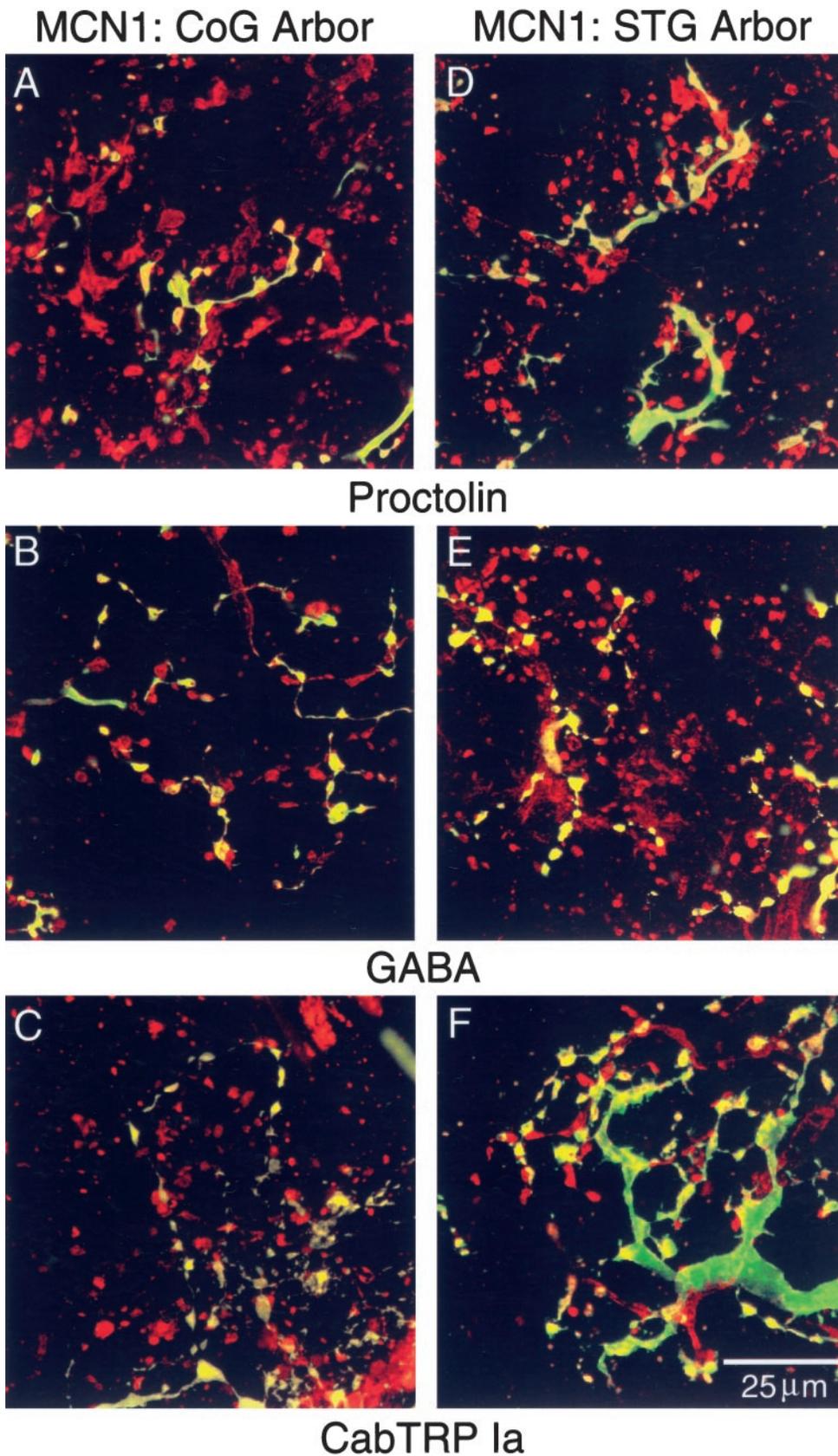
GABA

CabTRP Ia

Figure 3. The CoG and STG arbors of MCN1 contain proctolin, GABA, and CabTRP Ia. Confocal images of the MCN1 arbor in the CoG and STG demonstrate the MCN1 transmitter complement in each ganglion. In all panels, *green* represents LY, *red* represents antibody labeling, and *yellow* represents double labeling. *A–C*, Intracellular LY fill of MCN1 in the CoG. *D–F*, Intracellular LY fill of MCN1 in the STG. Intracellular fills are paired with proctolin immunocytochemistry (*A, D*), GABA immunocytochemistry (*B, E*), and CabTRP Ia immunocytochemistry (*C, F*). All panels show composite confocal images of eight optical sections taken at ~0.5 μm intervals, with the exception of *B,* which is a composite of four optical sections. Note: In many of the images shown here, there appears to be incomplete colocalization of dye and immunoreactivity. This is because nearly all modulator immunoreactivity in the neuropil is confined to varicose swellings present on the small-diameter terminal branches and is not always found within processes that connect these varicosities (Christie et al., 1997c).

Table 1. Transmitter complement of proctolin neurons

Transmitter	MCN1	MPN	MCN7
Proctolin	+	+	+
GABA	+	+	−
CabTRP	+	−	−

+, Immunopositive; −, immunonegative.

of the MPNs, we were able to conclude that these neurons are not immunoreactive for serotonin or histamine (Beltz et al., 1984; Katz et al., 1989; Christie, 1995) or TNRNFLRFamide, CabTRP Ia, red pigment-concentrating hormone-like, allatostatin-like, buccalin-like, myomodulin-like, or cholecystokinin-like peptides (Marder et al., 1987; Goldberg et al., 1988; Nusbaum and Marder, 1988; Christie et al., 1994, 1995, 1997c; Skiebe and Schneider, 1994).

MCN7 cotransmitter complement

MCN7 has a smaller-diameter axon than MCN1 as it enters the STG. Consequently, it is difficult to impale and fill the STG arbor of MCN7. Thus, all of our intracellular MCN7 fills are restricted to its CoG arbor. Pairing LY fills of MCN7 with proctolin immunocytochemistry demonstrated that MCN7 is proctolin-immunoreactive (Fig. 4*C1,C2*; *n* = 4). Because MCN1 and MPN are GABA-immunoreactive, we examined whether MCN7 is also GABA-immunoreactive. The confocal images in Figure 4, *D1* and *D2*, demonstrate that MCN7 is not GABA-immunoreactive (Table 1; *n* = 3). As indicated above, all of the CabTRP Ia immunoreactivity in the STG is from MCN1. Thus, MCN7 is not CabTRP Ia-immunoreactive (Table 1). Because all of the 5-HT immunoreactivity in the crab STG is from identified sensory neurons (Katz et al., 1989), MCN7 is not immunoreactive for 5-HT. We have not determined whether MCN7 contains any other transmitters.

Electrophysiology

The STG network produces the pyloric and gastric mill rhythms. We compared the influence of the three proctolin neurons in preparations in which the STG remained connected to the CoGs and OG via both the *son*s and *ion*s. Under these conditions, there is generally a relatively strong ongoing pyloric rhythm (~1 Hz) and occasionally an ongoing gastric mill rhythm. For all of the data presented here, the control condition consisted of an ongoing pyloric rhythm and no gastric mill rhythm.

MPN influence on the STG network

Nusbaum and Marder (1989a,b) demonstrated that, in preparations with the CoGs eliminated, MPN stimulation excites the pyloric rhythm. This includes an increase in pyloric cycle frequency and an increase in the activity level of several pyloric neurons. MPN never activated a gastric mill rhythm in those experiments. Nusbaum and Marder (1989a,b) were not able to study the MPN influence on ongoing gastric mill rhythms because, in the crab, the gastric mill rhythm is not spontaneously active when the CoGs are eliminated (Blitz et al., 1995; Bartos and Nusbaum, 1997; Weimann et al., 1997).

More recently, in preparations with the CoGs attached to the STG, Blitz and Nusbaum (1997) demonstrated that MPN stimulation still increases the activity level of several of the pyloric neurons. However, they did not examine the influence of MPN on either the pyloric cycle frequency or the phase relationships of the neurons participating in the motor pattern (see below). In our

present experiments, we found that in such preparations MPN stimulation (5–15 Hz) significantly increased the pyloric cycle frequency (1.01 ± 0.25 to 1.18 ± 0.21 Hz; paired Student's *t* test, *p* < 0.001; *n* = 13). MPN stimulation also increased the activity level of at least two of the pyloric neurons, the ventricular dilator (VD) and IC neurons (Fig. 5; *mvn*). In 35 of 35 preparations, MPN stimulation (5–15 Hz) did not elicit a gastric mill rhythm, which is evident in Figure 5 by the lack of rhythmic activity in the extracellular recordings of two gastric mill motor nerves (*lgn* and *dgn*). When there was an ongoing gastric mill rhythm, MPN stimulation inhibited this rhythm via its actions in the CoGs (Blitz and Nusbaum, 1997).

MCN1 influence on the STG network

Earlier work examined the influence of MCN1 stimulation on the STG network in preparations with the *son*s transected. Because all but two of the CoG neurons that innervate the STG project through the *son* instead of the *ion* (Coleman et al., 1992), this procedure eliminates most inputs to the STG. In the crab, the pyloric rhythm always slows and weakens, and sometimes terminates, when the *son*s are transected. This results from the removal of one or more spontaneously active projection neurons that provide continuous modulatory drive to the pyloric circuit neurons. With the *son*s transected, MCN1 excites the pyloric rhythm and activates a gastric mill rhythm (Coleman and Nusbaum, 1994; Bartos and Nusbaum, 1997). Bartos and Nusbaum (1997) found that MCN1 stimulation increases the pyloric cycle frequency, but this frequency is slower during one phase of the two-phase gastric mill rhythm, when the LG neuron is active. They showed that this is attributable to rhythmic presynaptic inhibition of the MCN1 terminals in the STG by the LG neuron (Coleman et al., 1995; Bartos and Nusbaum, 1997).

We found that when the CoGs remained connected to the STG via the *ion* and *son*, MCN1 stimulation elicited either of two gastric mill motor patterns. In 24 of 30 preparations, MCN1 stimulation (10–20 Hz) excited the pyloric rhythm and elicited the gastric mill rhythm shown in Figure 5. In these preparations, the elicited gastric mill rhythm resembled that elicited with the *son*s transected. This rhythm included alternating bursting in the LG and DG neurons and rhythmic LG-timed inhibition of the VD neuron (Fig. 5). This particular gastric mill rhythm has been designated the MCN1-elicited gastric mill rhythm (Blitz and Nusbaum, 1997). In 4 of 30 preparations, MCN1 stimulation elicited a gastric mill rhythm that differed from the MCN1-elicited gastric mill rhythm in several ways. For instance, the cycle frequency was slower, and both IC and VD activity were suppressed during each LG burst. This gastric mill rhythm is attributable to coactivity in MCN1 and another CoG projection neuron, called commissural projection neuron 2 (CPN2; Norris et al., 1994), and has been designated the MCN1/CPN2-elicited gastric mill rhythm (Blitz and Nusbaum, 1997). This rhythm results at least partly from MCN1 excitation of CPN2 within the CoG (D. M. Blitz and M. P. Nusbaum, unpublished observations). In the remaining 2 of 30 preparations, repeated stimulations of MCN1 elicited either the MCN1-elicited or the MCN1/CPN2-elicited gastric mill rhythm within the same preparation.

In all of these experiments, MCN1 stimulation also excited the pyloric rhythm. We analyzed the MCN1 excitation of the pyloric rhythm during times when the MCN1-elicited gastric mill rhythm was also active. Similar to preparations in which all other CoG influences were eliminated (Bartos and Nusbaum, 1997), MCN1 stimulation increased the pyloric cycle frequency but more so
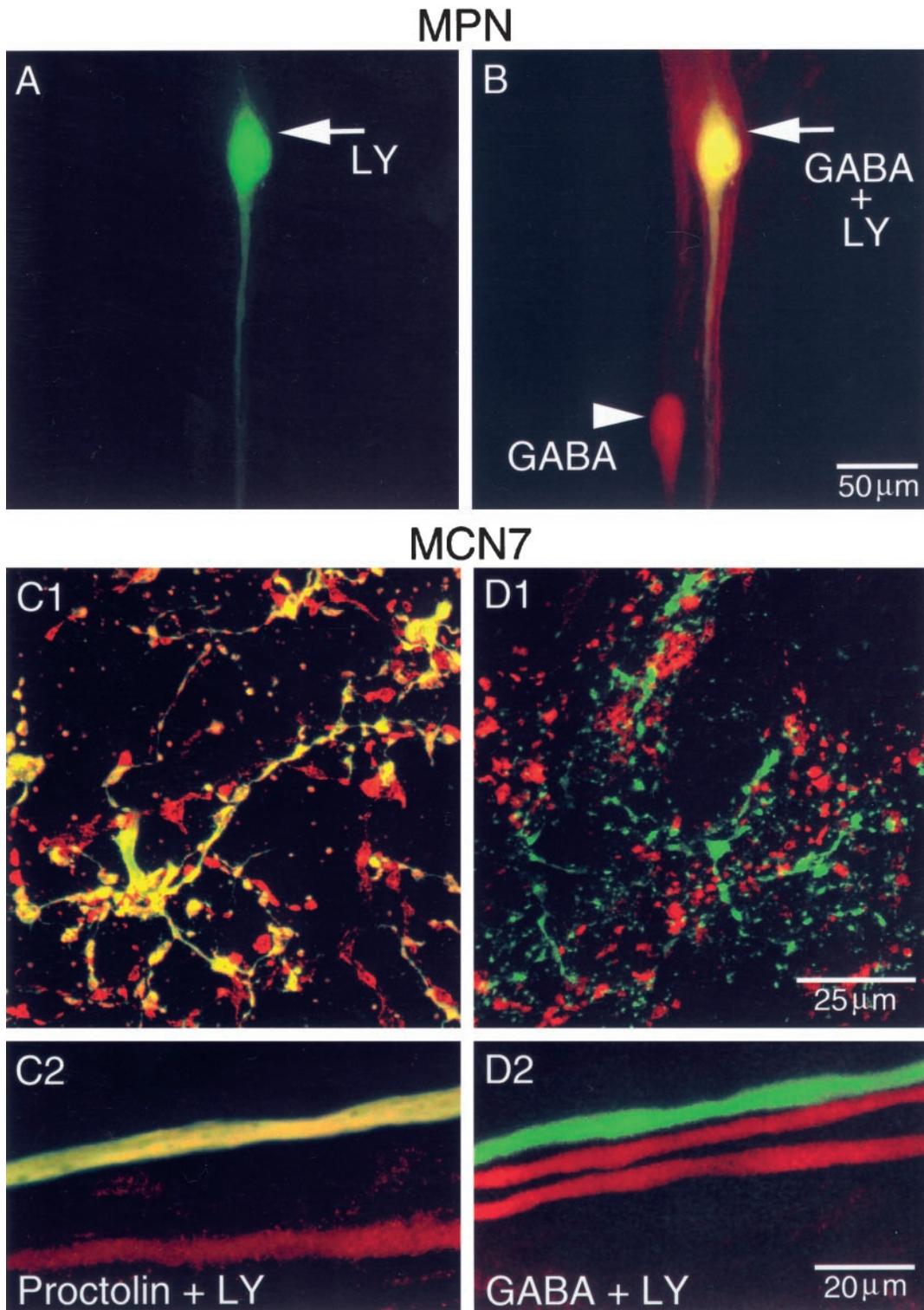
Figure 4. MPN contains proctolin (Nusbaum and Marder, 1989a) and GABA, whereas MCN7 contains proctolin but not GABA. In all panels, *green* represents LY, *red* represents antibody labeling, and *yellow* represents double labeling. *A,* Low-magnification view of an intracellular LY fill of MPN in the *on.* The *arrow* points to MPN soma. *B,* Same preparation processed for GABA immunocytochemistry. Note that the LY-filled soma (*arrow*) double labels for GABA immunoreactivity. The *arrowhead* indicates second MPN, which was not filled with LY but exhibits GABA immunoreactivity. *A* and *B* were collected simultaneously and are composite confocal images of 15 optical sections, each section being ∼2 μm thick. Scale bar is for both images. *C,* MCN7 is proctolin-immunoreactive. *C1,* High-magnification view of a region of a CoG neuropil from an intracellular LY fill of MCN7 paired with proctolin immunoctyochemistry. *C2,* High-magnification image of a region of the *son. C1* and *C2* are from the same preparation and are composite confocal images of 16 and 8 optical sections, respectively, taken at 0.5 μm intervals. *D,* MCN7 is not GABA-immunoreactive. *D1,* High-magnification confocal image of a region of CoG neuropil from an intracellular LY fill of MCN7 paired with GABA immunocytochemistry. *D2,* High-magnification image of a region of the *son* from the same preparation as *D1.* Confocal images are composites of eight optical sections taken at ∼0.5 μm intervals. Scale bar in *D1* is for *C1* and *D1.* Scale bar in *D2* is for *C2* and *D2.*
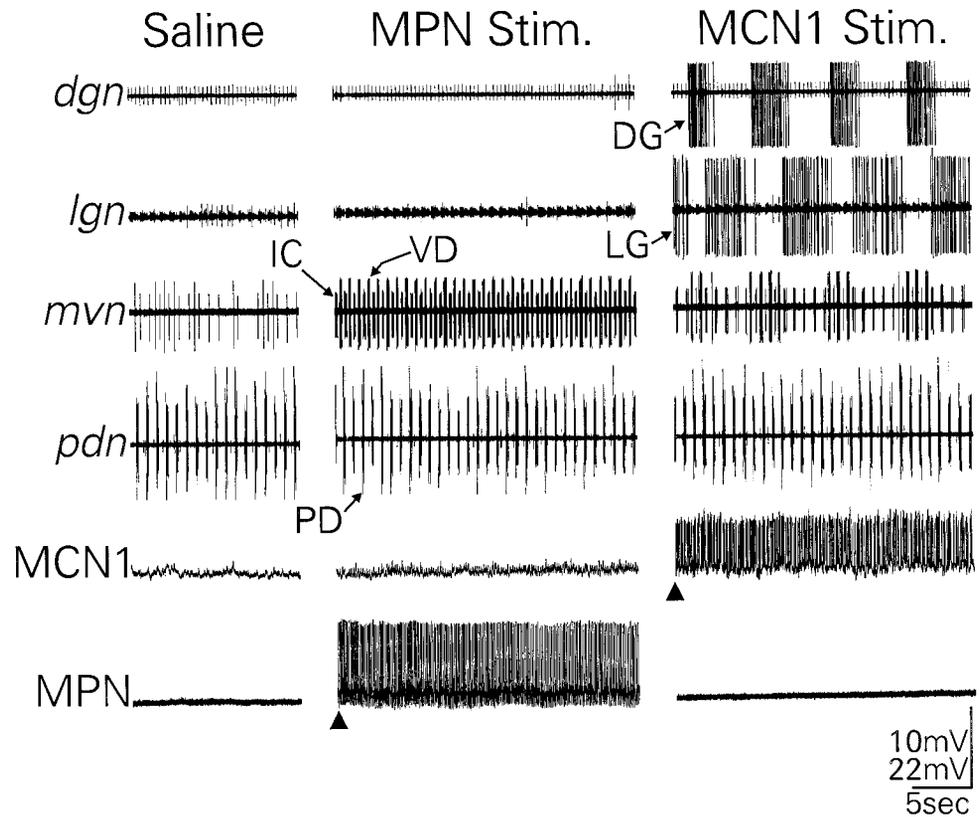
Figure 5. MPN and MCN1 elicit distinct STG motor patterns. *Left*, During saline superfusion and without any neuronal stimulation, there was an ongoing pyloric rhythm (*mvn*, *pdn*). There was no gastric mill rhythm (*dgn*, *lgn*). V_m: MPN, −72 mV; MCN1, −66 mV. *Middle*, When MPN was stimulated (9 Hz), there was an increase in the activity of IC and VD (*mvn*). MPN did not elicit a gastric mill rhythm (*dgn*, *lgn*). *Right*, When MCN1 was stimulated (11 Hz), a gastric mill rhythm was elicited, as is evident from the alternating bursting in the DG (*dgn*) and LG (*lgn*) neurons and the modified VD neuron pattern (*mvn*). This pattern is the MCN1-elicited gastric mill rhythm (Blitz and Nusbaum, 1997). MCN1 stimulation also caused increased activity in the IC and VD neurons.

during one of the two phases of the gastric mill rhythm. Specifically, MCN1 stimulation (10–20 Hz) elicited significant increases in pyloric cycle frequency during each retraction phase (DG burst) compared with the control pyloric frequency (1.05 ± 0.20 to 1.20 ± 0.21 Hz; one-way repeated measures ANOVA, Tukey t test, $p < 0.001$; $n = 12$). The pyloric frequency during each protraction phase (LG burst) was also significantly faster than prestimulation controls (1.05 ± 0.20 to 1.11 ± 0.19 Hz; one-way repeated measures ANOVA, Tukey t test, $p < 0.05$), but it was significantly slower than the cycle frequency during the retraction (DG) phase (one-way repeated measures ANOVA, Tukey t-test, $p < 0.001$).

MCN7 influence on the STG network

MCN7 stimulation elicited an STG motor pattern that differed considerably from that elicited by either MPN or MCN1. MCN7 stimulation (14–29 Hz) consistently caused the mean pyloric cycle frequency to decrease significantly (0.91 ± 0.26 to 0.81 ± 0.20 Hz; paired Student's t test, $p < 0.05$; $n = 17$) (Fig. 6). In Figure 6, the decreased pyloric frequency is particularly evident in the extracellular pyloric dilator nerve (*pdn*) recording, which displays the activity of the two PD neurons. The PD neurons are members of the pyloric pacemaker ensemble. During these longer pyloric cycles, there was a strong activation of the IC neuron, which produced long-duration bursts of action potentials (Fig. 6; $n = 20$). Note that there are long-duration IC neuron bursts interspersed with shorter-duration IC neuron bursts. These correlate with long- and short-duration pyloric cycles, respectively (see *pdn*). The intensity of VD neuron activity also increased (Fig. 6). In the same preparations, weaker MCN7 stimulation

(9–17 Hz) did not elicit the longer-duration IC bursts or decrease the pyloric cycle frequency ($n = 8$; data not shown). These stimulations elicited a slight increase in IC and VD activity and a slight increase in pyloric cycle frequency (0.89 ± 0.20 to 0.99 ± 0.13 Hz; paired Student's t test, $p < 0.05$; $n = 6$). We have designated the motor pattern resulting from the higher-frequency stimulations (14–29 Hz) the MCN7-elicited motor pattern.

The MCN7-elicited motor pattern also included activation of some gastric mill neurons. For example, during MCN7 stimulation, LG fired bursts of action potentials coincident with the longer-duration IC bursts (Fig. 6; $n = 18$). LG activity ranged from a few to many action potentials per burst, with intraburst firing frequencies of 3–12 Hz. The DG neuron displayed a more variable response, even within a single preparation. In 16 of 18 preparations, the DG neuron response to MCN7 stimulation was consistent during repeated stimulations. In these preparations, DG was co-active with LG and IC ($n = 4$ of 16), alternated with LG and IC ($n = 1$ of 16), fired irregularly ($n = 6$ of 16), or was silent ($n = 5$ of 16). In the other two preparations, the DG neuron was co-active or fired irregularly ($n = 1$) or was co-active or silent ($n = 1$) in response to repeated MCN7 stimulations within the same preparation. When activated by MCN7 stimulation, DG activity was fairly weak. Figure 6 demonstrates an example in which DG was primarily coactive with IC and LG, and it represents the high end of DG neuron activity during MCN7 stimulation.

The most striking characteristic of the MCN7-elicited motor pattern is the reduced pyloric cycle frequency associated with long-duration IC neuron bursts. We aimed to determine whether this was directly attributable to MCN7 inhibition of the pyloric pacemaker neurons, MCN7 actions on other pyloric neurons or a
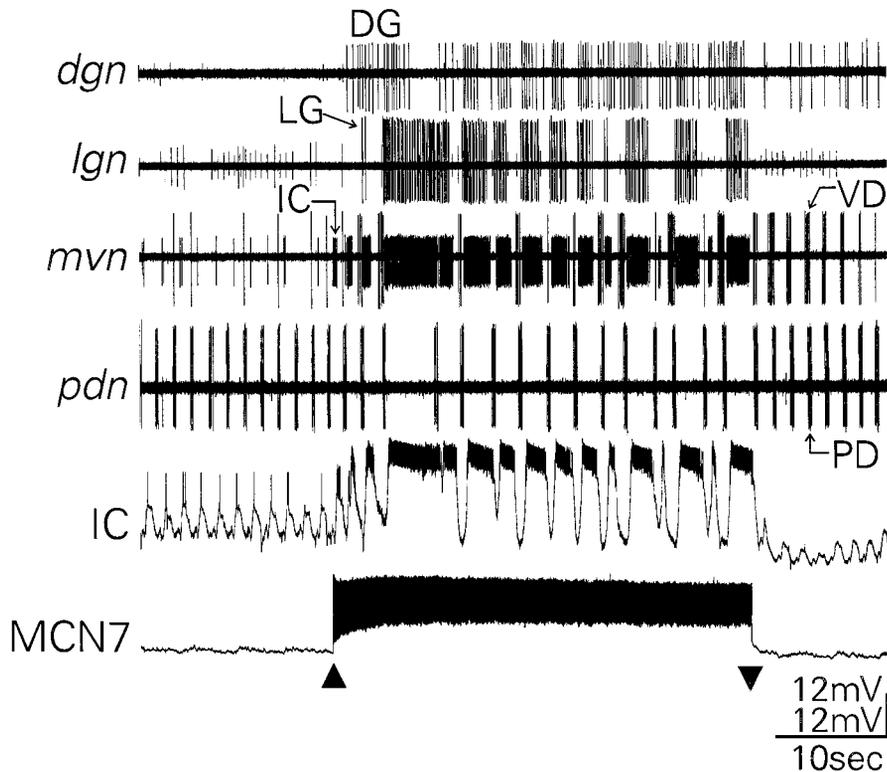
Figure 6. MCN7 elicits a distinct STG motor pattern. Before MCN7 stimulation, there was an ongoing pyloric rhythm (*IC, mvn, pdn*) and no gastric mill rhythm (*lgn, dgn*). When MCN7 was stimulated (23 Hz), the IC neuron was strongly excited, and the LG and DG neurons were activated. There was also a decrease in the average pyloric cycle frequency, which is most evident in the decreased frequency of the rhythmic PD neuron bursts (*pdn*). Note that the IC and LG neurons were coactive, whereas the DG neuron activity was less closely correlated to the activity of the other neurons. Most hyperpolarized V_m: MCN7, −65 mV; IC, −62 mV.

specific consequence of its excitation of the IC neuron. We found that IC was responsible for these events. In Figure 7, the pyloric rhythm was monitored with intracellular recordings of the IC and PD neurons. As shown above and in Figure 7*A*, the mean pyloric rhythm frequency was slower, and IC fired longer-duration bursts during MCN7 stimulation. These extended IC neuron bursts were always correlated with interruptions in the rhythmic PD oscillations and with the increased pyloric cycle durations. When we hyperpolarized the IC neuron and again stimulated MCN7, there was no inhibition evident in PD and no decrease in pyloric cycle frequency (Fig. 7*B*; n = 9). In fact, there was instead a small but significant increase in pyloric cycle frequency (1.00 ± 0.21 to 1.06 ± 0.21 Hz; paired Student's *t* test, p < 0.05). The pyloric cycle frequency elicited by MCN7 under this condition is significantly different from that elicited by MCN7 stimulation without hyperpolarization of the IC neuron (paired Student's *t* test, p < 0.05). When IC was released from hyperpolarization and MCN7 was stimulated, the pyloric frequency again decreased.

Hyperpolarization of the IC neuron had less influence on the gastric mill neuron responses to MCN7. In five of nine preparations, the LG neuron response to MCN7 stimulation was similar with or without IC hyperpolarization. In the other four preparations, LG activity was slightly weaker. At times when the DG neuron was activated by MCN7 stimulation (n = 6 of 9), DG activity was either weaker (n = 3 of 6) or unchanged (n = 3 of 6) during hyperpolarization of IC.

Although all three proctolin projection neurons increase IC neuron activity (Nusbaum and Marder, 1989b; Bartos and Nusbaum, 1997; Blitz and Nusbaum, 1997; this study), only MCN7 elicited the long-duration IC bursts and the resulting decreased pyloric cycle frequency. In addition, MCN7 only had this effect when its firing frequency was >14 Hz (see above). One possible

explanation for why MCN7 had a stronger influence on the IC neuron is that MCN7 might release more proctolin onto the IC neuron than do MPN and MCN1 when these neurons fire within the same firing frequency range. Perhaps, if MPN and MCN1 released more proctolin, they would also elicit the longer-duration bursts in the IC neuron. We tested this possibility by stimulating MPN and MCN1 at faster firing frequencies.

In response to intracellular current injection, MPN fired at a maximal frequency of 30 Hz. This level of MPN activity did not elicit the longer-duration IC neuron bursts, and there was no decrease in pyloric cycle frequency (n = 4). We were able to stimulate each MCN1 extracellularly via the *ion* (see Materials and Methods) at 30 Hz for a combined maximal firing frequency of 60 Hz. To be certain that each MCN1 was firing at 30 Hz, we recorded the LG neuron intracellularly. LG receives electrical EPSPs from MCN1 (Coleman et al., 1995). By triggering an oscilloscope sweep with each stimulus, we determined that there was a time-locked compound EPSP in LG elicited by the coincident action potentials in the two MCN1 neurons (n = 6). Under these conditions, MCN1 stimulation did not elicit the longer-duration IC neuron bursts, and there was no decrease in pyloric cycle frequency (n = 6).

Distinct motor patterns elicited by proctolin neurons

We have described the major distinctions in the three proctolin neuron motor patterns. That is, MPN elicits a pyloric motor pattern, MCN1 elicits a gastropyloric motor pattern, and MCN7 elicits a slower pyloric motor pattern that is dominated by IC neuron bursts. The MCN7 motor pattern also incorporates a neuron, LG, normally associated with the gastric mill rhythm. To further characterize the differences among these three motor patterns, we performed a quantitative comparison of the pyloric
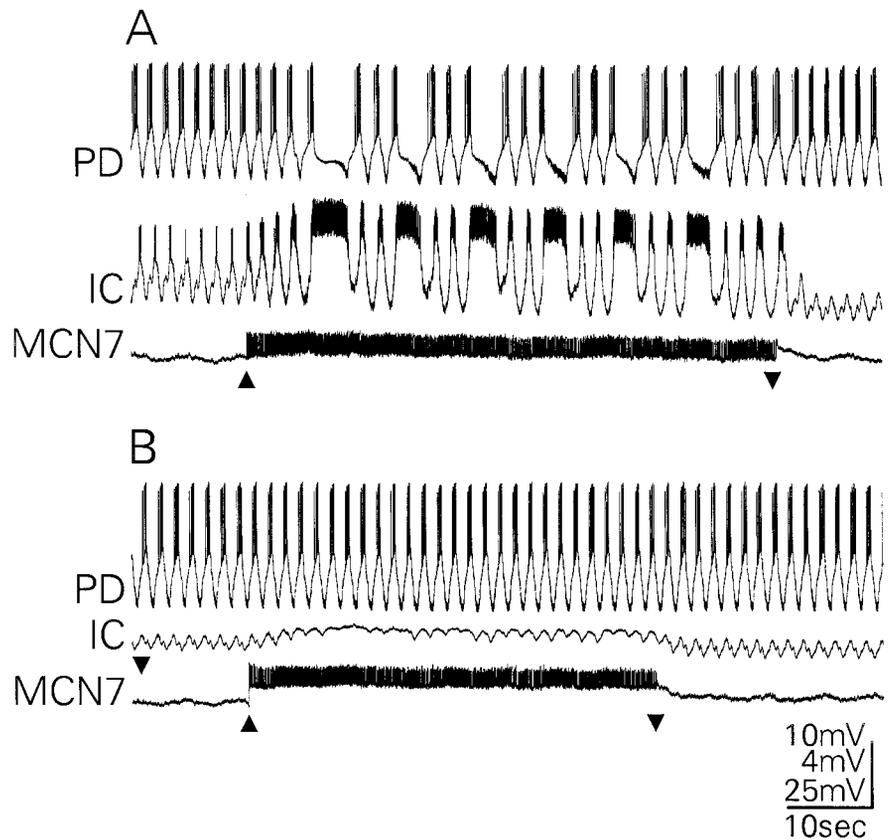
Figure 7. MCN7 excitation of the IC neuron causes a decreased pyloric cycle frequency. *A*, MCN7 stimulation (21 Hz) excited IC and caused a decrease in pyloric frequency, evident in the periodic decrease in frequency of PD neuron bursts. Note the extended period of hyperpolarization in PD during each extended IC burst. PD is one of the pyloric pacemaker neurons. *B*, When IC was hyperpolarized with constant-amplitude negative current and MCN7 was again stimulated (21 Hz), there was no decrease in pyloric cycle frequency. Current injections were via explicitly unbalanced bridge circuits.

component of each motor pattern. First, we determined whether there was a significant difference in the pyloric cycle frequency elicited by each proctolin neuron. The pyloric cycle frequency elicited by MCN7 stimulation is significantly different from that elicited by MPN stimulation (one way ANOVA, Tukey *t* test, $p < 0.001$). The pyloric cycle frequency elicited by MCN7 stimulation is also significantly different from the pyloric cycle frequency elicited by MCN1 stimulation during the LG ($p < 0.001$) and DG ($p < 0.001$) phases (one way ANOVA, Tukey *t* test). There were no significant differences among the control pyloric cycle frequencies occurring before stimulation of each proctolin neuron.

To characterize further the pyloric component of the three proctolin neuron motor patterns, we performed phase analyses on three pyloric neurons that are active for at least a portion of each motor pattern. This analysis allowed us to compare the relative onset, offset, and duty cycle of the PD, IC, and VD neurons within a pyloric cycle. Duty cycle is defined as the portion of a cycle during which a neuron is active. For the MCN1 motor pattern, we performed a separate phase analysis for the retraction (DG) and protraction (LG) phases of the gastric mill rhythm (see Materials and Methods). Also, for the MCN7 motor pattern we analyzed short-duration pyloric cycles separately from long-duration cycles. Short-duration cycles were identified as those in which the cycle duration was <1 SD above the mean control cycle duration. Long-duration cycles were those longer than the mean + 1 SD of the control cycle duration (see Materials and Methods). Figure 8 illustrates that there are several significant differences between the motor patterns elicited by each of the three proctolin neurons. Figure 8, *left panels*, shows phase diagrams for each pattern, and the *asterisks* in the *right panels* denote statisti-

cally significant differences between the corresponding pattern on the left and the other four motor patterns.

The most dramatic differences between the motor patterns involved the IC neuron. For example, during long-duration MCN7 cycles, the IC neuron duty cycle was greater than in any other condition (Fig. 8) ($n = 4$ preparations for each condition). This was mostly attributable to a significant phase delay in IC neuron burst offset during this motor pattern. During the MCN1 motor pattern, the IC neuron was not active during every pyloric cycle. Specifically, the IC neuron was active during only 18 of 40 pyloric cycles occurring during the DG phase of the gastric mill rhythm. When IC was active at these times, its duty cycle was shorter than during any of the other four motor patterns (Fig. 8). This resulted from significant differences in both IC neuron burst onset and offset compared with those occurring in the other motor patterns. The PD neuron offset was more similar than for IC activity across all motor patterns, although it occurred significantly later during both phases of the MCN1 pattern compared with the MPN or MCN7 patterns (Fig. 8). The VD neuron was active during every cycle (40 of 40) of each motor pattern except the MCN7 long-duration cycles (10 of 40 pyloric cycles) and the MCN1-LG phase cycles (10 of 40 pyloric cycles). Moreover, during the latter condition, VD neuron burst onset occurred significantly later than during MCN7 short duration cycles or MCN1-DG phase cycles. There were no differences in VD neuron offset during MCN1, MPN, or MCN7 stimulation (Fig. 8). Also noteworthy in Figure 8 is that the only pair of pyloric motor patterns that exhibited no significant differences between them were the MCN7 short-duration cycles and the MPN motor pattern.
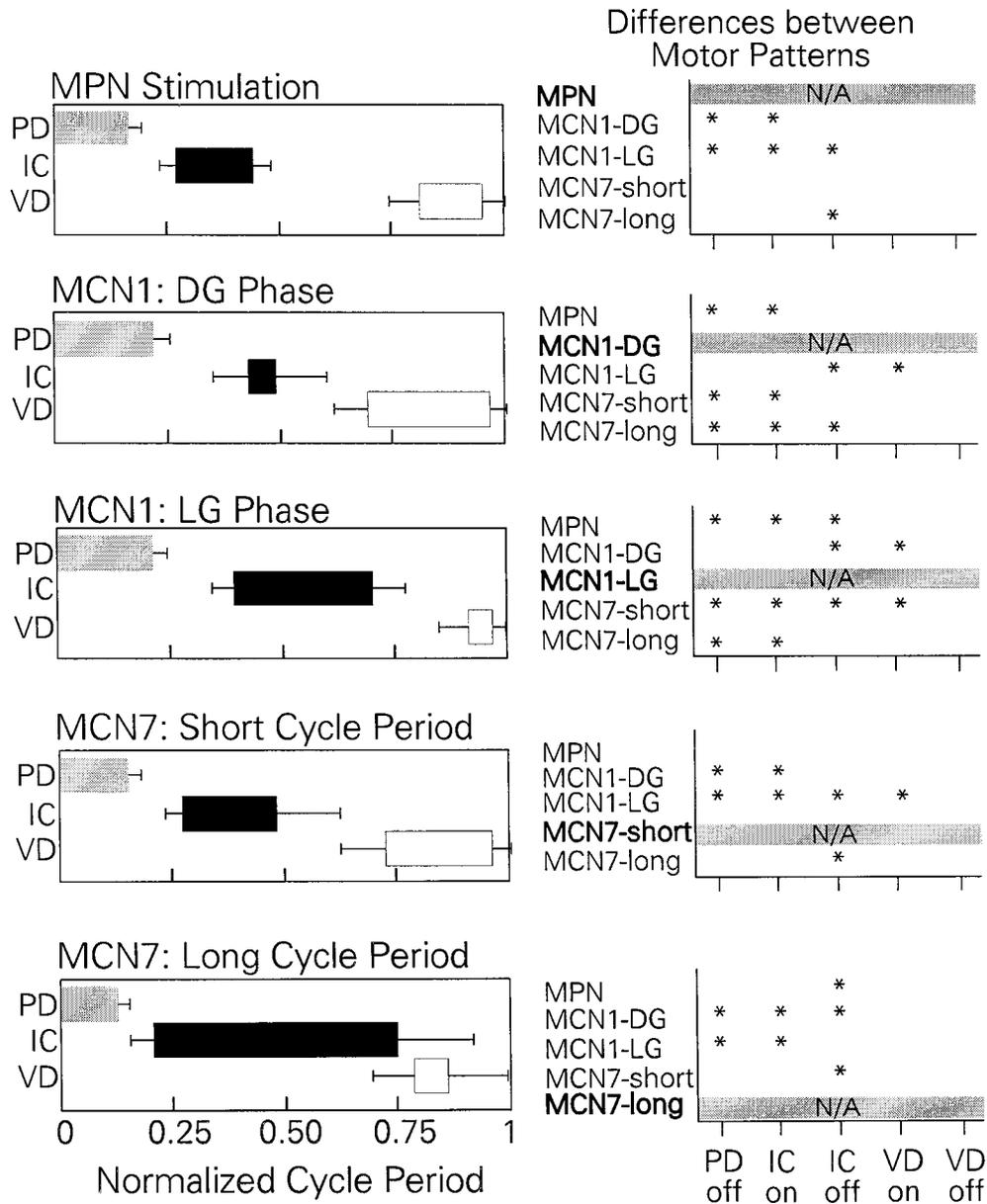
Figure 8. Selective stimulation of MPN, MCN1, or MCN7 elicits different pyloric motor patterns. *Left*, The mean ± SD phase of burst onset and offset for the PD, IC, and VD neurons during a pyloric cycle is plotted during MPN, MCN1, and MCN7 stimulation. One pyloric cycle was arbitrarily designated as beginning with the onset of a PD neuron burst (phase = 0) and ending with the onset of the next PD burst (phase = 1). Pyloric cycles during MCN1 stimulation were divided into those occurring during either the retraction (DG neuron burst) or the protraction (LG neuron burst) half of the gastric mill rhythm. Pyloric cycles during MCN7 stimulation were divided into short- and long-duration cycles. Short-duration cycles are those that are shorter than the mean + 1 SD of the control pyloric cycle period before stimulation. Long-duration cycles are those longer than 1 SD above the mean control pyloric cycle period before stimulation. For each of the five conditions shown, 10 cycles per preparation were measured from four preparations. During MCN1-DG phase pyloric cycles, the IC neuron was not always active. Thus there were only 18 total measurements for this parameter. During MCN7 long-duration cycles and MCN1-LG phase cycles, there are only 10 total measurements each of VD phase onset and offset, because the VD neuron was often silent during these patterns. For details of analysis, see Materials and Methods. *Right*, For each parameter (e.g., PD neuron burst offset, IC neuron burst onset) a one-way ANOVA was conducted followed by multiple comparisons using the Tukey *t* test. *Asterisks* represent significant differences. For IC neuron burst onset and offset, all significant differences represent $p < 0.001$. For PD and VD phase, significant differences range from $p < 0.05$ to $p < 0.001$.

It remained possible that the different motor patterns elicited by MPN, MCN1, and MCN7 were attributable to variability between preparations. To test this possibility, we sequentially stimulated more than one of these neurons in the same preparation. Under these conditions, we compared the STG response to stimulation of MPN and MCN1 (26 preparations) (see Fig. 5), MPN and MCN7 (6 preparations), MCN1 and MCN7 (11 preparations), or all three proctolin neurons (2 preparations). In all

cases, MPN elicited the pyloric motor pattern, MCN1 elicited the gastropyloric pattern, and MCN7 elicited the pyloric pattern dominated by IC bursts described above.

DISCUSSION

This study demonstrates that modulatory projection neurons can have a neuropeptide transmitter in common and still elicit distinct motor patterns from a common target network. We have found
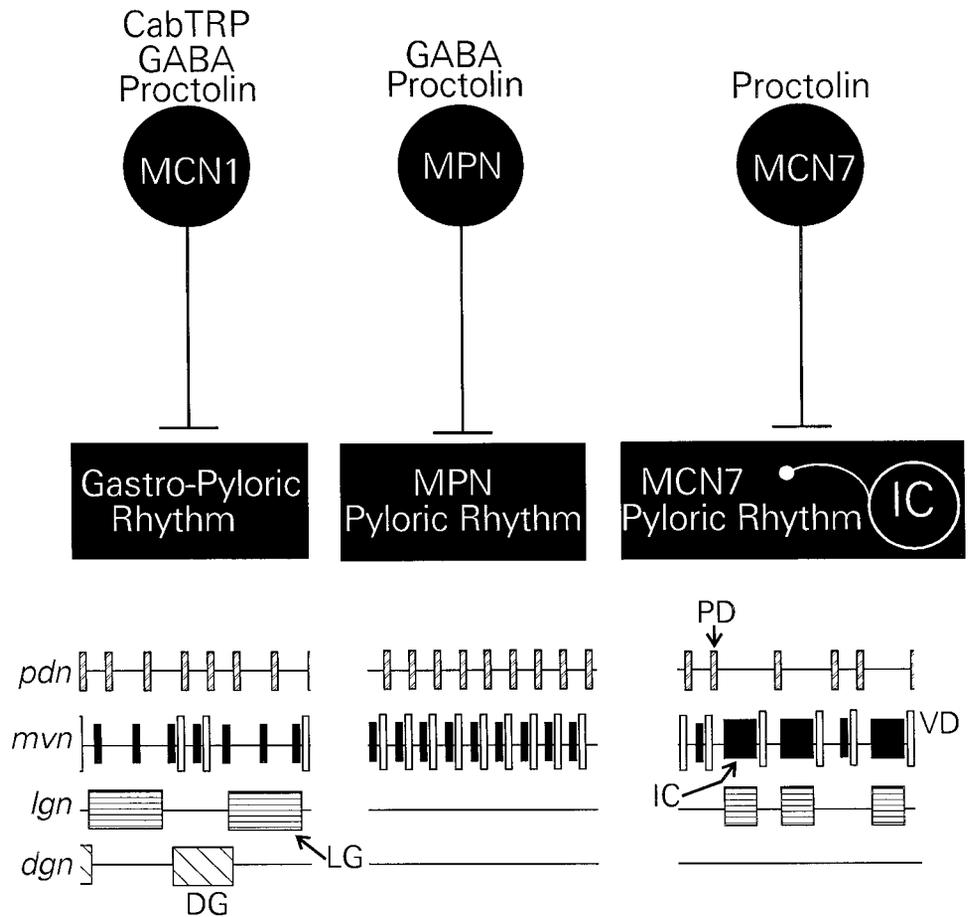
Figure 9. Summary of the distinct motor patterns elicited from the crab STG network by selective activation of the proctolin neurons MCN1, MPN, and MCN7. *Top,* MCN1 contains the transmitters CabTRP Ia, GABA, and proctolin, and it elicits a gastropyloric motor pattern. MPN contains proctolin and GABA but not CabTRP Ia. It elicits a particular pyloric rhythm and no gastric mill rhythm. MCN7 contains proctolin but not GABA and CabTRP Ia. MCN7 elicits a distinct pyloric motor pattern, which is dominated by IC neuron bursts. During this motor pattern, IC neuron activity regulates the pyloric frequency. *Bottom,* Schematic representation of the motor patterns elicited by MCN1, MPN, and MCN7. *Boxes* represent bursts of action potentials in an individual neuron.

that there are three modulatory projection neurons that innervate the crab STG and contain the same peptide transmitter. However, each of these neurons contains a distinct cotransmitter complement and elicits distinct motor patterns from the STG network (Fig. 9). MCN1 stimulation selects a gastric mill rhythm and a modified pyloric rhythm. MPN and MCN7 stimulation select distinct pyloric motor patterns without activation of the gastric mill rhythm. The pyloric rhythm elicited by MCN7 is significantly slower, because of the enhanced activity of a pyloric circuit neuron. A gastric mill neuron is also incorporated into this latter rhythm.

In many systems, it has proven difficult to locate and/or manipulate neural network inputs. Thus, techniques such as exogenous application of modulatory transmitters (Harris-Warrick et al., 1992b; McCormick, 1992; Pearson, 1993; Aston-Jones et al., 1996; Ramirez and Richter, 1996; Sillar et al., 1997) and the simultaneous activation of groups of input neurons (Aston-Jones et al., 1996; Grillner et al., 1997; Lalley et al., 1997; Wannier et al., 1998) are commonly used to study modulation of network activity in vertebrate and invertebrate systems. Information from such studies suggests a shared role for multiple input neurons that contain the same modulatory transmitter and influence the same behavior (McCormick, 1992; Aston-Jones et al., 1996; Page and Sofroniew, 1996; Edwards and Kravitz, 1997; Jacobs and Fornal, 1997). Although the actions of individual modulatory neurons on multifunctional networks have been studied in several systems (Pearson, 1993; Marder and Calabrese, 1996), there are few preparations in which the transmitters of these neurons have been catalogued so that a comparison of the effects of bath-applied and

neurally released transmitter can be made. In the few preparations in which this has been possible, there are some instances in which bath application does indeed mimic neuronal activity (Kuhlman et al., 1985; Nusbaum and Marder, 1989b; McCrohan and Croll, 1997). However, this may be the exception rather than the rule. As demonstrated here, populations of same transmitter-containing neurons that project to a common target network can represent a heterogeneous population. We show that three input neurons with the same peptide transmitter elicit distinct motor patterns from their target network. It is likely that these different motor patterns result at least partially from the unique complement of cotransmitters in each of these proctolin neurons (Wood and Nusbaum, 1998). In other systems as well, there do not appear to be common pairings or groupings of cotransmitters in multiple-transmitter neurons (Walker and Holden-Dye, 1991; Furness et al., 1992; Zupanc, 1996).

In addition to having distinct cotransmitter complements, the three proctolin neurons each use other distinct strategies to elicit their respective STG motor patterns. For instance, one of the unique aspects of the MPN motor pattern is its suppression of the gastric mill rhythm (Blitz and Nusbaum, 1997). MPN inhibits the gastric mill rhythm via its actions in the CoGs, where it inhibits projection neurons (MCN1 and CPN2) that activate the gastric mill rhythm (Blitz and Nusbaum, 1997). MCN1 also influences other projection neurons. When the CoGs remain connected to the STG, MCN1 stimulation elicits the MCN1/CPN2-elicited gastric mill rhythm in some preparations. This results at least partly from MCN1 excitation of CPN2 within the CoGs (Blitz and Nusbaum, unpublished observations). Although in some sys-

tems it has been demonstrated that parallel inputs can act independently (Juranek and Metzner, 1998), it is likely that interactions among parallel inputs are not unique to the crab stomatogastric system (Brodfeuhrer and Burns, 1995; Faumont et al., 1996). The synaptic actions of a projection neuron that occur onto parallel pathways outside of the target network would not be mimicked by bath application to a neuronal network.

MCN1 stimulation elicits a pyloric rhythm that differs from the MPN and MCN7 pyloric rhythms. This is partly attributable to MCN1 also eliciting a gastric mill rhythm, which alters the activity of some pyloric neurons because they participate in both the pyloric and gastric mill rhythms. For example, during the MCN1-elicited motor pattern, the IC and VD neurons display activity patterns linked to both the pyloric and gastric mill rhythms. Both their level of activity and their phase relationships differ during the two gastric mill phases (see Figs. 5, 8). Additionally, the gastric mill rhythm regulates MCN1 excitation of the pyloric rhythm (Coleman and Nusbaum, 1994; Bartos and Nusbaum, 1997; this study). This regulation occurs via presynaptic inhibition from the LG neuron onto the STG terminals of MCN1 (Coleman et al., 1995). There are no such interactions involving LG and either MCN7 or MPN. Presynaptic regulation of input neuron activity occurs in many neural networks, although the function of these presynaptic actions has only been identified in a few systems (Nusbaum, 1994; Nusbaum et al., 1997; Lomeli et al., 1998). There can be no presynaptic inhibition of bath-applied transmitter. Not surprisingly then, the STG response to MCN1 stimulation is not the same as co-applying the MCN1 transmitters (Christie et al., 1997b; D. E. Wood and M. P. Nusbaum, unpublished observations).

In addition to the strategies discussed above, some aspects of the motor patterns elicited by the three proctolin neurons result from their actions on different populations of STG target neurons. For example, only MCN1 and MCN7 excite the LG and DG neurons. However, the proctolin neurons also have different influences on common target neurons. For instance, all three proctolin neurons excite the IC neuron, but the actions of MCN7 on IC are considerably stronger than those of MPN and MCN1. The dramatic change in IC neuron activity elicited by MCN7 may be attributable to an as yet unidentified cotransmitter in MCN7. Supporting this possibility is the fact that, in preparations with the CoG inputs eliminated, bath-applied proctolin (10^{-6} M) increases the pyloric cycle frequency and excites the IC neuron, but IC does not fire long-duration bursts (Nusbaum and Marder, 1989b). Furthermore, IC does not cause a decrease in pyloric cycle frequency when excited by MPN or MCN1 stimulation, even when they fire at frequencies above those of MCN7. However, the actions of applied proctolin and stimulation of MPN or MCN1 include excitation of other pyloric neurons that inhibit the IC neuron (Nusbaum and Marder, 1989a; Bartos and Nusbaum, 1997; Blitz and Nusbaum, 1997). This may limit IC neuron burst duration and intensity. Therefore, an alternative possibility to an unidentified cotransmitter is that MCN7 might have a stronger or more selective proctolin-mediated influence on the IC neuron. In support of this possibility, our phase analysis demonstrates that the short-duration pyloric cycles during MCN7 stimulation are similar to the MPN motor pattern that is mimicked by bath-applied proctolin (Nusbaum and Marder, 1989b). Thus, MCN7 may elicit its motor pattern by using a higher concentration of proctolin to influence the IC neuron than its other target neurons. This might be mediated by increased proctolin release near the proctolin receptors on the IC neuron, a higher proctolin receptor

concentration on IC near MCN7 release sites, and/or a lower density of proctolin-cleaving peptidases (Coleman et al., 1994) in the region of MCN7 release sites that influence IC. Also supporting a role for proctolin in the IC neuron response to MCN7 stimulation is an *in vivo* study by Heinzel et al. (1993) in *C. pagurus* in which proctolin application (10^{-6} M) elicited a motor pattern similar to that elicited by MCN7 stimulation *in vitro*.

Under usual conditions, the IC neuron plays little or no role in setting the pyloric rhythm frequency (Hooper and Marder, 1987). Nevertheless, in response to MCN7 stimulation, the IC neuron strongly influences pyloric cycle frequency. This is likely to be a result of MCN7 altering the IC neuron membrane properties and/or its synaptic actions. Modulation of these properties is a well documented mechanism for altering neural network activity in many systems (Katz and Frost, 1995; Marder and Calabrese, 1996; Calabrese and Feldman, 1997; McDearmid et al., 1997; Ayali et al., 1998).

Previous work dissecting the neural network response to neuropeptide application concluded that it is equally important to document which network components are and are not direct targets of peptide action (Hooper and Marder, 1987). Similarly, with respect to understanding the response of a multifunctional network to neurally released peptide, it is evident that issues such as cotransmission, compartmentalization of peptide action, local interactions with network neurons, and interactions among parallel inputs must be considered. These issues increase the complexity of transmitter action and demonstrate the diversity that can exist in the function of a single neurotransmitter. There is still much to be learned about the mechanisms that allow different neurons with the same peptide transmitter to have distinct actions on network activity. Future work aimed at understanding the cellular details of such mechanisms will enable us to gain greater understanding of how multifunctional neural networks obtain their considerable flexibility.

REFERENCES

Aston-Jones G, Rajkowski J, Kubiak P, Valentino RJ, Shipley MT (1996) Role of the locus coeruleus in emotional activation. Prog Brain Res 107:379–402.

Ayali A, Johnson BR, Harris-Warrick RM (1998) Dopamine modulates graded and spike-evoked synaptic inhibition independently at single synapses in pyloric network of lobster. J Neurophysiol 79:2063–2069.

Bartos M, Nusbaum MP (1997) Intercircuit control of motor pattern modulation by presynaptic inhibition. J Neurosci 17:2247–2256.

Beltz BS, Kravitz EA (1983) Mapping of serotonin-like immunoreactivity in the lobster nervous system. J Neurosci 3:585–602.

Beltz B, Eisen JS, Flamm R, Harris-Warrick RM, Hooper SL, Marder E (1984) Serotonergic innervation and modulation of the stomatogastric ganglion of three decapod crustaceans (*Panulirus interruptus*, *Homarus americanus* and *Cancer irroratus*). J Exp Biol 109:35–54.

Bishop CA, O'Shea M, Miller RJ (1981) Neuropeptide proctolin (H-Arg-Tyr-Leu-Pro-Thr-OH): immunological detection and neuronal localization in insect central nervous system. Proc Natl Acad Sci USA 78:5899–5902.

Blitz DM, Nusbaum MP (1997) Motor pattern selection via inhibition of parallel pathways. J Neurosci 17:4965–4975.

Blitz DM, Christie AE, Marder E, Nusbaum MP (1995) Distribution and effects of two families of tachykinin-like peptides in the stomatogastric nervous system of the crab, *Cancer borealis*. J Comp Neurol 354:282–294.

Brezina V, Weiss KR (1997) Analyzing the functional consequences of transmitter complexity. Trends Neurosci 20:538–543.

Brodfuehrer PD, Burns A (1995) Neuronal factors influencing the decision to swim in the medicinal leech. Neurobiol Learn Mem 63:192–199.

Calabrese RL, Feldman JL (1997) Intrinsic membrane properties and synaptic mechanisms in motor rhythm generators. In: Neurons, networks and motor behavior (Stein PSG, Grillner S, Selverston AI, Stuart DG, eds), pp 119–130. Cambridge, MA: MIT.

Christie AE (1995) Chemical neuroanatomy of the crab stomatogastric ganglion: a study using immunocytochemistry and laser scanning confocal microscopy. PhD Thesis, Brandeis University.

Christie AE, Norris BJ, Coleman MJ, Marder E, Nusbaum MP (1993) Neuropil arborization and transmitter complement of a modulatory projection neuron. Soc Neurosci Abstr 19:931.

Christie AE, Hall C, Oshinsky M, Marder E (1994) Buccalin-like and myomodulin-like peptides in the stomatogastric ganglion of the crab *Cancer borealis*. J Exp Biol 193:337–343.

Christie AE, Baldwin D, Turrigiano G, Graubard K, Marder E (1995) Immunocytochemical localization of multiple cholecystokinin-like peptides in the stomatogastric nervous system of the crab *Cancer borealis*. J Exp Biol 198:263–271.

Christie AE, Lundquist CT, Nässel DR, Nusbaum MP (1997a) Two novel tachykinin-related peptides from the nervous system of the crab *Cancer borealis*. J Exp Biol 200:2279–2294.

Christie AE, Wood DE, Nusbaum MP (1997b) A neuromodulatory role for *Cancer borealis* tachykinin-related peptide Ia in the crab stomatogastric ganglion. Soc Neurosci Abstr 23:476.

Christie AE, Baldwin DH, Marder E, Graubard K (1997c) Organization of the stomatogastric neuropil of the crab, *Cancer borealis*, as revealed by modulator immunocytochemistry. Cell Tissue Res 288:135–148.

Coleman MJ, Nusbaum MP (1994) Functional consequences of compartmentalization of synaptic input. J Neurosci 14:6544–6552.

Coleman MJ, Nusbaum MP, Cournil I, Claiborne BJ (1992) Distribution of modulatory inputs to the stomatogastric ganglion of the crab, *Cancer borealis*. J Comp Neurol 325:581–594.

Coleman MJ, Norris BJ, Nusbaum MP (1993) Functional modification of rhythmic motor activity by a modulatory projection neuron. Soc Neurosci Abstr 19:1701.

Coleman MJ, Konstant PH, Rothman BS, Nusbaum MP (1994) Neuropeptide degradation produces functional inactivation in the crustacean nervous system. J Neurosci 14:6205–6216.

Coleman MJ, Meyrand P, Nusbaum MP (1995) A switch between two modes of synaptic transmission mediated by presynaptic inhibition. Nature 378:502–505.

Davis NT, Velleman SG, Kingan TG, Keshishian H (1989) Identification and distribution of a proctolin-like neuropeptide in the nervous system of the gypsy moth, *Lymantria dispar*, and in other Lepidoptera. J Comp Neurol 283:71–85.

Edwards DH, Kravitz EA (1997) Serotonin, social status and aggression. Curr Opin Neurobiol 7:812–819.

Faumont S, Simmers J, Meyrand P (1996) Stabilizing control of a motor pattern generating network via interacting higher order modulatory interneurons. Soc Neurosci Abstr 22:132.

Furness JB, Bornstein JC, Murphey R, Pompolo S (1992) Roles of peptides in transmission in the enteric nervous system. Trends Neurosci 15:66–71.

Goldberg D, Nusbaum MP, Marder E (1988) Substance P-like immunoreactivity in the stomatogastric nervous systems of the crab *Cancer borealis* and the lobsters *Panulirus interruptus* and *Homarus americanus*. Cell Tissue Res 252:515–522.

Grillner S, Georgopoulos AP, Jordan LM (1997) Selection and initiation of motor behavior. In: Neurons, networks and motor behavior (Stein PSG, Grillner S, Selverston AI, Stuart DG, eds), pp 3–19. Cambridge, MA: MIT.

Harris-Warrick RM, Marder E, Selverston A, Moulins M eds (1992a) Dynamic biological networks: the stomatogastric nervous system. Cambridge, MA: MIT.

Harris-Warrick RM, Nagy F, Nusbaum MP (1992b) Neuromodulation of stomatogastric networks by identified neurons and transmitters. In: Dynamic biological networks: the stomatogastric nervous system (Harris-Warrick RM, Marder E, Selverston AI, Moulins M, eds), pp 87–137. Cambridge, MA: MIT.

Heinzel H, Weimann JM, Marder E (1993) The behavioral repertoire of the gastric mill of the crab, *Cancer pagurus*: an *in situ* endoscopic and electrophysiological examination. J Neurosci 13:1793–1803.

Hooper SL, Marder E (1987) Modulation of the lobster pyloric rhythm by the peptide proctolin. J Neurosci 7:2097–2112.

Jacobs BL, Fornal CA (1997) Serotonin and motor activity. Curr Opin Neurobiol 7:820–825.

Juranek J, Metzner W (1998) Segregation of behavior-specific synaptic inputs to a vertebrate neuronal oscillator. J Neurosci 18:9010–9019.

Katz PS, Frost WN (1995) Intrinsic neuromodulation in the *Tritonia* swim CPG: the serotonergic dorsal swim interneurons act presynaptically to enhance transmitter release from interneuron C2. J Neurosci 15:6035–6045.

Katz PS, Eigg MH, Harris-Warrick RM (1989) Serotonergic/cholinergic muscle receptor cells in the crab stomatogastric nervous system. I. Identification and characterization of the gastropyloric receptor cells. J Neurophysiol 62:558–570.

Kuhlman JR, Li C, Calabrese RL (1985) FMRF-amide-like substances in the leech. II. Bioactivity on the heartbeat system. J Neurosci 5:2310–2317.

Lalley PM, Benacka R, Bischoff AM, Richter DW (1997) Nucleus raphe obscurus evoked 5HT-1A receptor mediated modulation of respiratory neurons. Brain Res 747:156–159.

Lomeli J, Quevedo J, Linares P, Rudomin P (1998) Local control of information flow in segmental and ascending collaterals of single afferents. Nature 395:600–604.

Lundberg JM (1996) Pharmacology of cotransmission in the autonomic nervous system: integrative aspects on amines, neuropeptides, adenosine triphosphate, amino acids and nitric oxide. Pharmacol Rev 48:113–178.

Madsen AJ, Herman WS, Elde R (1985) Differential distribution of two homologous neuropeptides (RPCH and AKH) in the crayfish nervous system. Soc Neurosci Abstr 11:941.

Marder E, Calabrese RL (1996) Principles of rhythmic motor pattern generation. Physiol Rev 76:687–717.

Marder E, Hooper SL, Siwicki KK (1986) Modulatory action and distribution of the neuropeptide proctolin in the crustacean stomatogastric nervous system. J Comp Neurol 243:454–467.

Marder E, Calabrese RL, Nusbaum MP, Trimmer B (1987) Distribution and partial characterization of FMRFamide-like peptides in the stomatogastric nervous systems of the rock crab, *Cancer borealis*, and the spiny lobster, *Panulirus interruptus*. J Comp Neurol 259:150–163.

Marder E, Jorge-Rivera JC, Kilman V, Weimann JM (1997) Peptidergic modulation of synaptic transmission in a rhythmic motor system. Adv Organ Biol 2:213–233.

McCormick DA (1992) Neurotransmitter actions in the thalamus and cerebral cortex and their role in neuromodulation of thalamocortical activity. Prog Neurobiol 39:337–388.

McCrohan CR, Croll RP (1997) Characterization of an identified cerebrobuccal neuron containing the neuropeptide APGWamide (Ala-Pro-Gly-Trp-NH$_2$) in the snail *Lynmaea stagnalis*. Invert Neurosci 2:273–283.

McDearmid JR, Scrymgeour-Wedderburn JF, Sillar KT (1997) Aminergic modulation of glycine release in a spinal network controlling swimming in *Xenopus laevis*. J Physiol (Lond) 503:111–117.

Mulloney B, Hall WM (1991) Neurons with histamine-like immunoreactivity in the segmental and stomatogastric nervous systems of the crayfish *Pacifastacus leniusculus* and the lobster *Homarus americanus*. Cell Tissue Res 266:197–207.

Norekian TP, Satterlie RA (1996) Cerebral serotonergic neurons reciprocally modulate swim and withdrawal neural networks in the mollusk *Clione limacina*. J Neurophysiol 75:538–546.

Norris BJ, Coleman MJ, Nusbaum MP (1994) Recruitment of a projection neuron determines gastric mill motor pattern selection in the stomatogastric nervous system of the crab, *Cancer borealis*. J Neurophysiol 72:1451–1463.

Norris BJ, Coleman MJ, Nusbaum MP (1996) Pyloric motor pattern modification by a newly identified projection neuron in the crab stomatogastric nervous system. J Neurophysiol 75:97–108.

Nusbaum MP (1994) Presynaptic control of neurones in pattern-generating networks. Curr Opin Neurobiol 4:909–914.

Nusbaum MP, Kristan Jr WB (1986) Swim initiation in the leech by serotonin-containing interneurons, cells 21 and 61. J Exp Biol 122:277–302.

Nusbaum MP, Marder E (1988) A neuronal role for a crustacean red pigment concentrating hormone-like peptide: Neuromodulation of the pyloric rhythm in the crab, *Cancer borealis*. J Exp Biol 135:165–181.

Nusbaum MP, Marder E (1989a) A modulatory proctolin-containing neuron (MPN). I. Identification and characterization. J Neurosci 9:1591–1599.

Nusbaum MP, Marder E (1989b) A modulatory proctolin-containing neuron (MPN). II. State-dependent modulation of rhythmic motor activity. J Neurosci 9:1600–1607.

Nusbaum MP, Cournil I, Golowasch J, Marder E (1989) Modulating

rhythmic motor activity with a proctolin- and GABA-containing neuron. Soc Neurosci Abstr 15:366.

Nusbaum MP, Weimann JM, Golowasch J, Marder E (1992) Presynaptic control of modulatory fibers by their neural network targets. J Neurosci 12:2706–2714.

Nusbaum MP, El Manira A, Gossard J-P, Rossignol S (1997) Presynaptic mechanisms during rhythmic activity in vertebrates and invertebrates. In: Neurons, networks and motor behavior (Stein PSG, Grillner S, Selverston AI, Stuart DG, eds), pp 237–253. Cambridge, MA: MIT.

Page KJ, Sofroniew MV (1996) The ascending basal forebrain cholinergic system. Prog Brain Res 107:513–522.

Pearson KG (1993) Common principles of motor control in vertebrates and invertebrates. Annu Rev Neurosci 16:265–297.

Perrins R, Weiss KR (1996) A cerebral central pattern generator in *Aplysia* and its connections with buccal feeding circuitry. J Neurosci 16:7030–7045.

Ramirez JM, Richter DW (1996) The neuronal mechanisms of respiratory rhythm generation. Curr Opin Neurobiol 6:817–825.

Saleh TM, Kombian SB, Zidichouski JA, Pittman QJ (1996) Peptidergic modulation of synaptic transmission in the parabrachial nucleus *in vitro*: importance of degradative enzymes in regulating synaptic efficacy. J Neurosci 16:6046–6055.

Schmidt M, Ache BW (1994) Descending neurons with dopamine-like or with substance P/FMRFamide-like immunoreactivity target the somata of olfactory interneurons in the brain of the spiny lobster, *Panulirus argus*. Cell Tissue Res 278:337–352.

Sigvardt KA, Rothman BS, Brown RO, Mayeri E (1986) The bag cells of *Aplysia* as a multitransmitter system: identification of alpha bag cell peptide as a second neurotransmitter. J Neurosci 6:803–813.

Sillar KT, Kiehn O, Kudo N (1997) Chemical modulation of vertebrate motor circuits. In: Neurons, networks and motor behavior (Stein PSG, Grillner S, Selverston AI, Stuart DG, eds), pp 183–193. Cambridge, MA: MIT.

Skiebe P, Schneider H (1994) Allatostatin peptides in the crab stomatogastric nervous system: inhibition of the pyloric motor pattern and distribution of allatostatin-like immunoreactivity. J Exp Biol 194:195–208.

Thorogood MSE, Brodfuehrer PD (1995) The role of glutamate in swim initiation in the medicinal leech. Invert Neurosci 1:223–233.

Vilim FS, Cropper EC, Price DA, Kupfermann I, Weiss KR (1996) Release of peptide cotransmitters in *Aplysia*: regulation and functional implications. J Neurosci 16:8092–8104.

Walker RJ, Holden-Dye L (1991) Evolutionary aspects of transmitter molecules, their receptors and channels. Parasitology 102:S7–S29.

Wannier T, Deliagina TG, Orlovsky GN, Grillner S (1998) Differential effects of the reticulospinal system on locomotion in lamprey. J Neurophysiol 80:103–112.

Weimann JM, Marder E (1994) Switching neurons are integral members of multiple oscillatory networks. Curr Biol 4:896–902.

Weimann JM, Meyrand P, Marder E (1991) Neurons that form multiple pattern generators: Identification and multiple activity patterns of gastric/pyloric neurons in the crab stomatogastric system. J Neurophysiol 65:111–112.

Weimann JM, Marder E, Evans B, Calabrese RL (1993) The effects of SDRNFLRFamide and TNRNFLRFamide on the motor patterns of the stomatogastric ganglion of the crab, *Cancer borealis*. J Exp Biol 181:1–26.

Weimann JM, Skiebe P, Heinzel HG, Soto C, Kopell N, Jorge-Rivera JC, Marder E (1997) Modulation of oscillator interactions in the crab stomatogastric ganglion by crustacean cardioactive peptide. J Neurosci 17:1748–1760.

Weiss KR, Brezina V, Cropper EC, Heierhorst J, Hooper SL, Probst WC, Rosen SC, Vilim FS, Kupfermann I (1993) Physiology and biochemistry of peptidergic cotransmission in *Aplysia*. J Physiol (Lond) 87:141–151.

Wood DE, Nusbaum MP (1998) Different modulatory neurons elicit distinct circuit responses despite common co-transmitters. Soc Neurosci Abstr 23:1890.

Zupanc GKH (1996) Peptidergic transmission: from morphological correlates to functional implications. Micron 27:35–91.